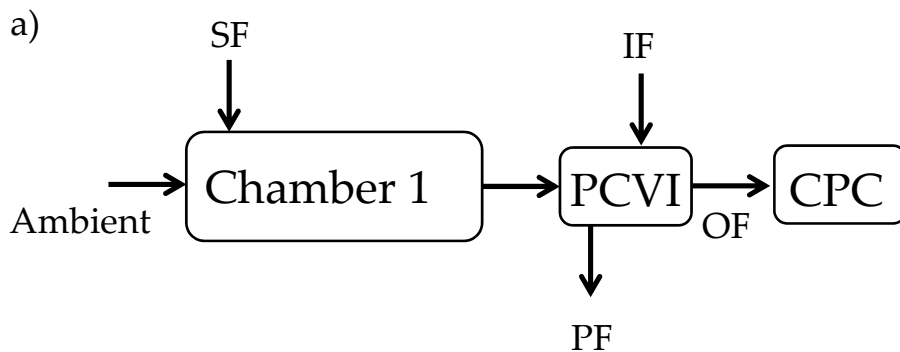


**CFD model details:**

CFD simulations were performed using commercial available CFD software ANSYS FLUENT. The solver was pressure based Navier stoked equation, steady state with implicit and absolute velocity formulation. RNG  $\kappa - \epsilon$  turbulence model with energy and viscous heating enable species transport model was used. The pressure calculations were performed using Standard model settings. Also, pressure-velocity coupling was based on default SIMPLE model.

**Table S1:** Temperature dependent water droplet breakthrough limits for chamber 1 and 2.

Temperature (°C)		-26	-28	-30	-32	-34
Breakthrough limit (RH <sub>w</sub> )	Chamber 1	~112%	~114%	>115%	>115%	>115%
	Chamber 2	>115%	>115%	>115%	>115%	>115%



b)

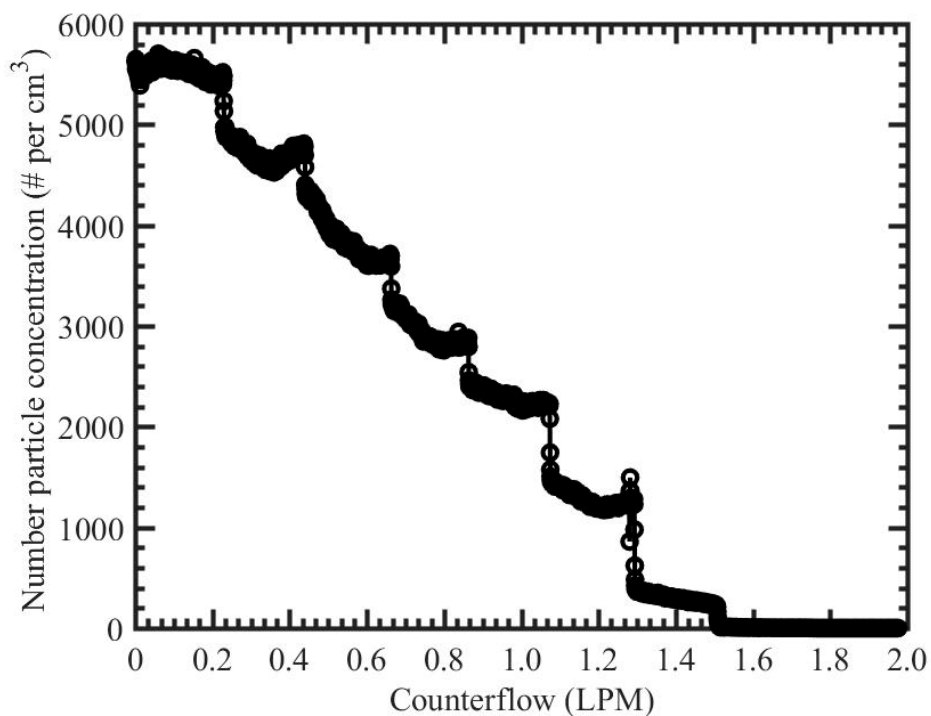


**Figure S1:** a) Experimental setup to investigate the threshold counterflow of PCVI. b) Number concentration of ambient particles transmitted through the PCVI with increasing counterflow during flow calibration. CPC: condensation particle counter; IF: Input Flow; PF: Pump Flow; OF: Output Flow. PCVI flows were: inlet flow = 10.0 LPM; IF = 2.8 LPM; PF = 11.8 LPM; and OF was 1.0 LPM. IF is divided into counterflow and OF, for details see Kulkarni et al. (2011).

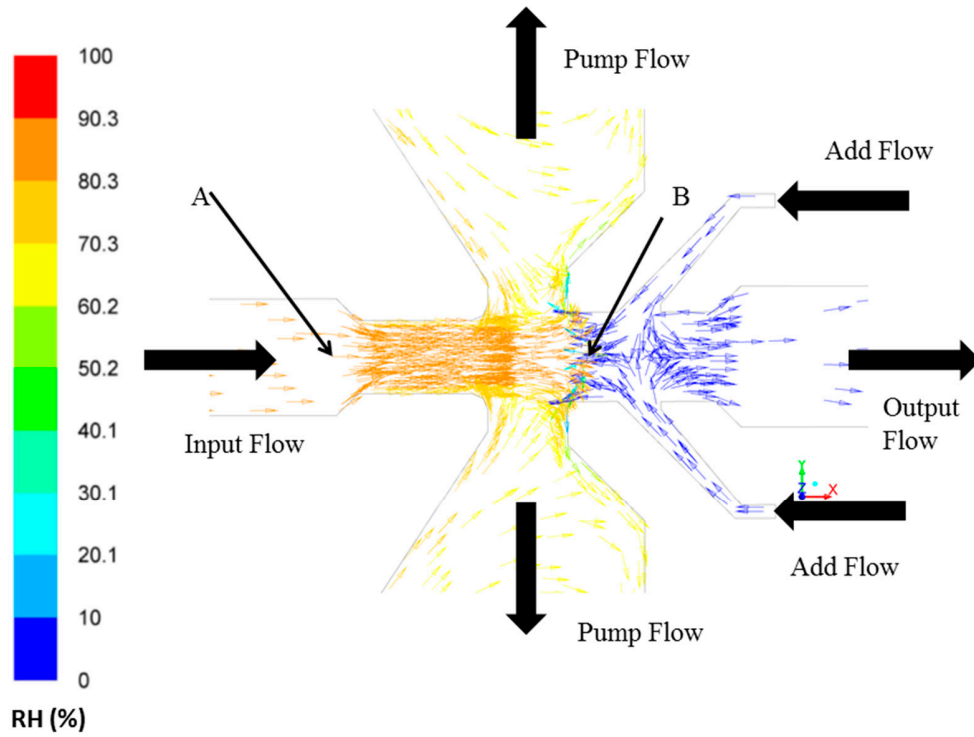


**Figure S2:** Velocity vectors colored by RH within the PCVI. Label A shows the location where input flow begins to increase, and label B shows the first stagnation plane. The RH and velocity magnitudes corresponding to these locations are shown in Figure S3. This figure implies large ice crystals transmitted through the PCVI are exposed to dry cold temperature air conditions (RH = 0% and -30 °C) that helps to sublimate the ice crystals in the output flow.

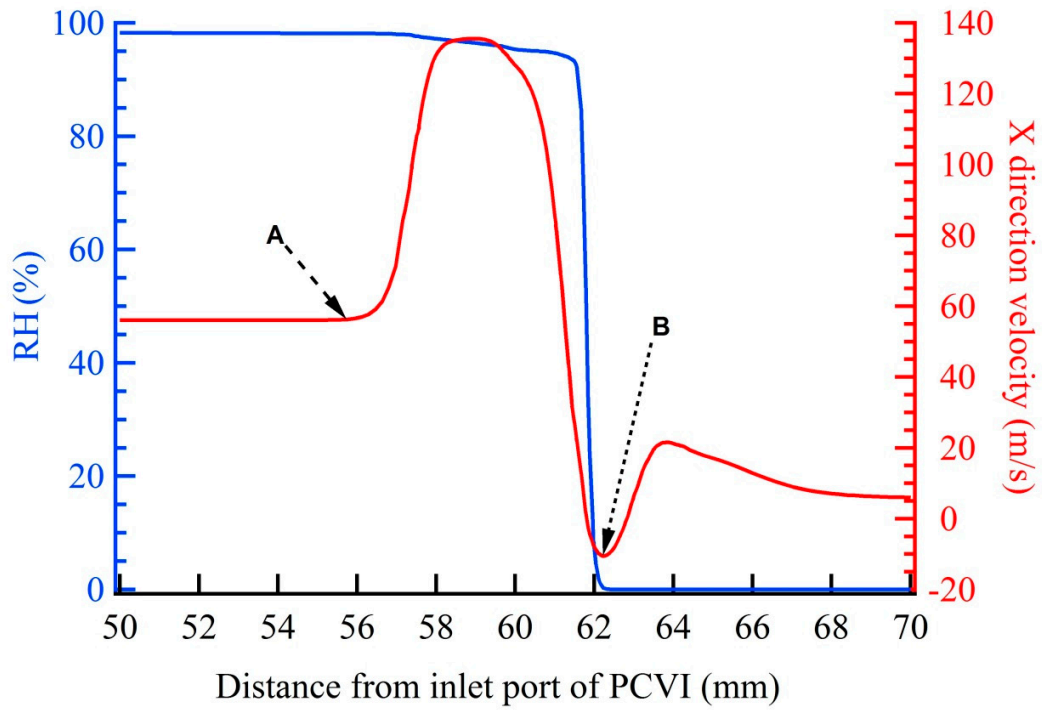


**Figure S3:** Traces of relative humidity (RH) and velocity magnitudes within the PCVI (in the axial direction). More details on labels A and B are shown in Figure S2.

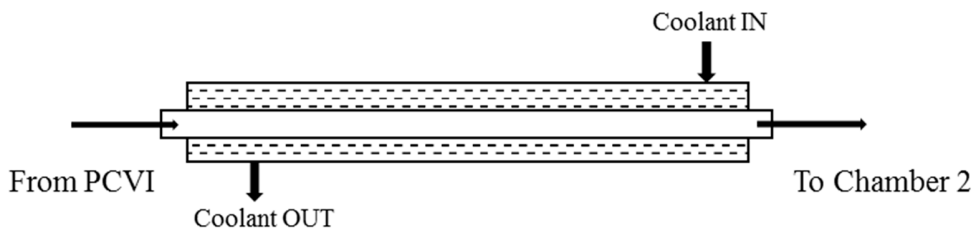


**Figure S4:** Schematic of the heat exchanger. The exchanger consists of two concentric cylinders. The function of inner cylinder is to sublimate the ice crystals and connects the output port of PCVI to the inlet port of the ice chamber 2. The outer cylinder carries the heat transfer coolant that maintain the heat exchanger unit at  $-30^{\circ}\text{C}$ .

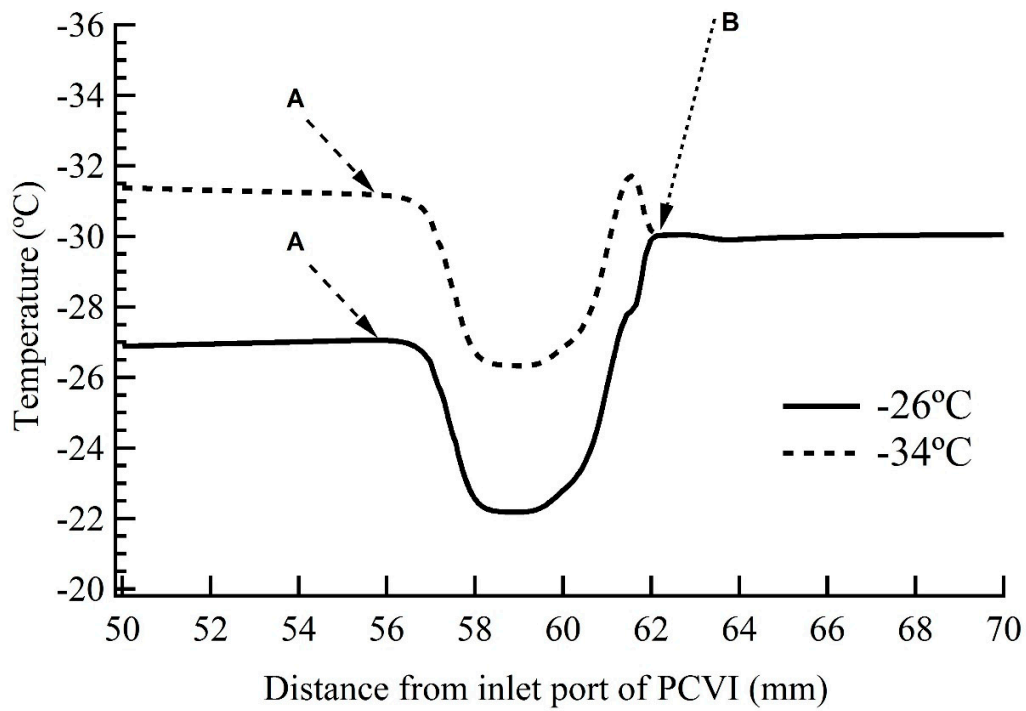


**Figure S5:** Traces of air temperature within the PCVI (in the axial direction) suggesting output flow port temperature condition (-30°C) is insensitive to the input flow temperature conditions (-26 and -34°C: the temperature conditions from the experiment, see section 3.2). More details on labels A and B are shown in Figure S2.

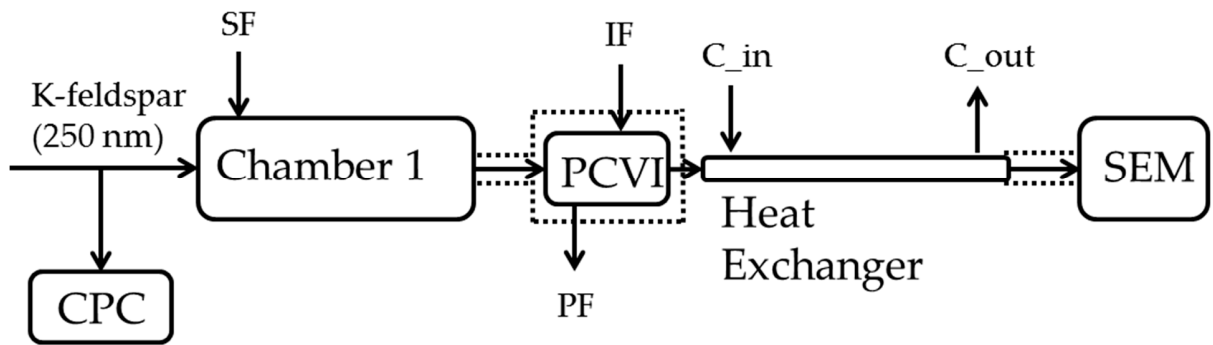


**Figure S6:** Experiment set-up to understand the size-distribution of ice residuals. K-feldspar particles of 250 nm in mobility diameter were transported to the chamber 1 and ice residuals were collected on single stage impactor using Lacey support film. Figure notations are same as Figure 1.

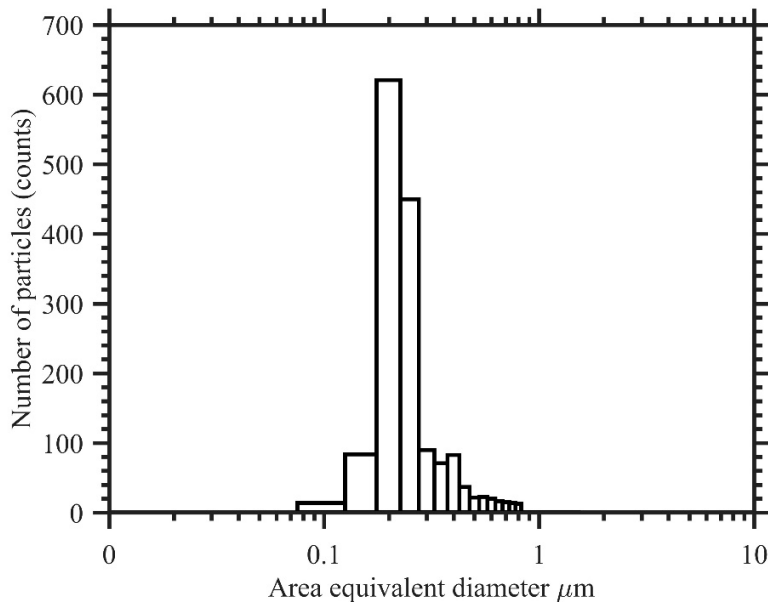


**Figure S7:** Size-distribution of ice residuals through SEM analysis. See Figure S6 for more details.

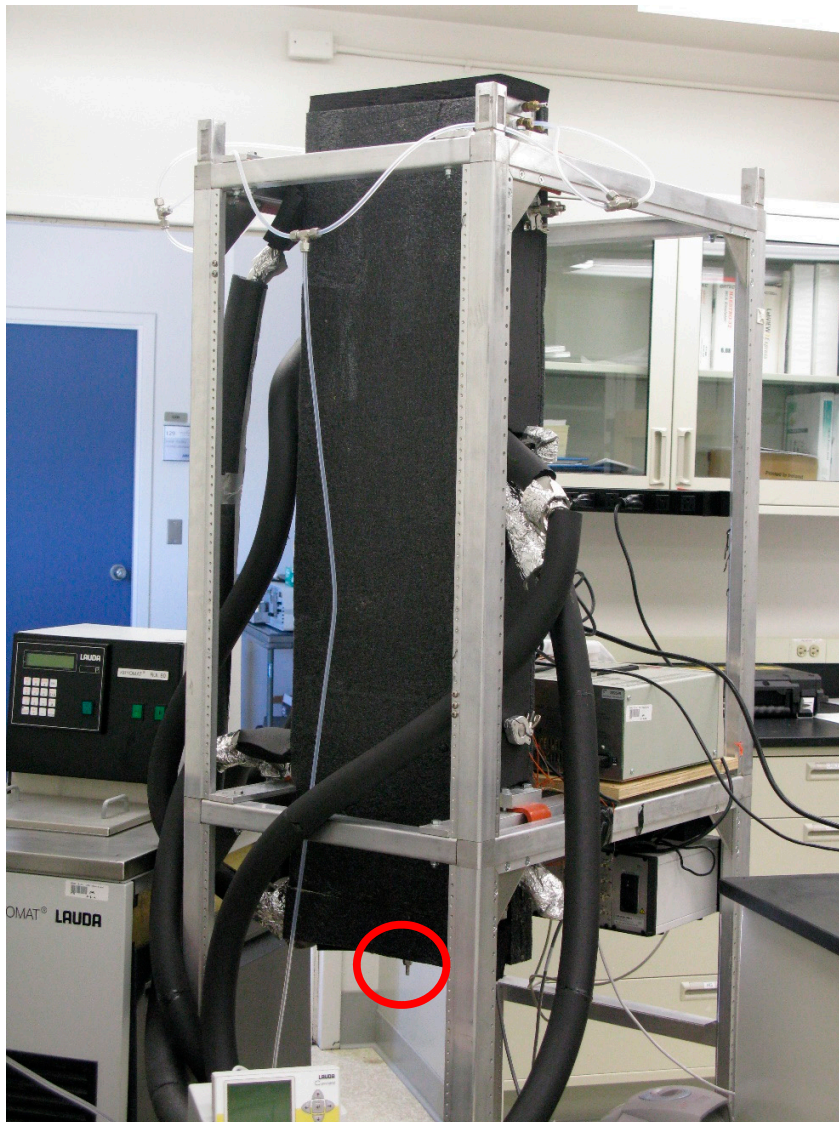


**Figure S8:** Photograph of the chamber 1 as described in Figure 1. The highlighted red circle shows the exit port of the chamber. To this port PCVI and heat exchanger units are connected. The exit of the heat exchanger is connected to the chamber 2, shown in Figure S9.



**Figure S9:** Photograph of the chamber 2 as described in Figure 1. Highlighted unit of the chamber shows the inlet port.

**References:**

Kulkarni, G., et al., *Comparison of Experimental and Numerical Studies of the Performance Characteristics of a Pumped Counterflow Virtual Impactor*. *Aerosol Science and Technology*, 2011. **45**(3): p. 382-392.